REVIEW

OPEN

Current emerging MRI tools for radionecrosis and pseudoprogression diagnosis

Lucia Nichelli[a,b] *and Stefano Casagranda*[c]

Purpose of review
This review aims to cover current MRI techniques for assessing treatment response in brain tumors, with a focus on radio-induced lesions.

Recent findings
Pseudoprogression and radionecrosis are common radiological entities after brain tumor irradiation and are difficult to distinguish from real progression, with major consequences on daily patient care. To date, shortcomings of conventional MRI have been largely recognized but morphological sequences are still used in official response assessment criteria. Several complementary advanced techniques have been proposed but none of them have been validated, hampering their clinical use. Among advanced MRI, brain perfusion measures increase diagnostic accuracy, especially when added with spectroscopy and susceptibility-weighted imaging. However, lack of reproducibility, because of several hard-to-control variables, is still a major limitation for their standardization in routine protocols. Amide Proton Transfer is an emerging molecular imaging technique that promises to offer new metrics by indirectly quantifying intracellular mobile proteins and peptide concentration. Preliminary studies suggest that this noncontrast sequence may add key biomarkers in tumor evaluation, especially in posttherapeutic settings.

Summary
Benefits and pitfalls of conventional and advanced imaging on posttreatment assessment are discussed and the potential added value of APT in this clinicoradiological evolving scenario is introduced.

Keywords
advanced MRI, amide proton transfer weighted imaging, brain tumor, pseudoprogression, radionecrosis

INTRODUCTION

MRI plays a key-role in brain tumor follow-up, allowing to monitor response to treatment or the detection of progression, and therefore, driving critical clinical decisions. From year to year, as the therapeutic arsenal increases, assessing treatment efficacy, especially after radiotherapy or during immunotherapy, becomes more difficult. The distinction between pseudoprogression and radionecrosis from true progression or stable disease is often not possible with conventional MRI sequences and requires advanced imaging. However, no advanced MRI protocol has yet been validated. The aim of this article is to review the current knowledge on the posttherapeutic evaluation of brain tumors with a focus on the potential added value of Amide Proton Transfer (APT), a new promising noncontrast MRI technique belonging to Chemical Exchange Saturation Transfer (CEST) imaging domain.

[a]Department of Neuroradiology, Sorbonne Université, Assistance Publique-Hôpitaux de Paris, Groupe Hospitalier Pitié-Salpêtrière-Charles Foix, [b]Sorbonne Université, INSERM, CNRS, Assistance Publique-Hôpitaux de Paris, Institut du Cerveau et de la Moelle épinière, boulevard de l'Hôpital, Paris and [c]Department of Research & Innovation, Olea Medical, avenue des Sorbiers, La Ciotat, France

Correspondence to Lucia Nichelli, MD, Department of Neuroradiology, Groupe Hospitalier Pitié-Salpêtrière-Charles Foix, boulevard de l'Hôpital, Paris, France. Tel: +33 1 42 16 35 96; e-mail: lucia.nichelli@aphp.fr

Curr Opin Oncol 2021, 33:597–607

DOI:10.1097/CCO.0000000000000793

KEY POINTS

- Brain radionecrosis and pseudo progression require advanced imaging.
- Perfusion holds the higher diagnostic accuracy, especially when combined with spectroscopy and susceptibility-weighted imaging.
- Diffusion weighted imaging must be interpreted with caution, as similar diffusion water molecules metric can reflect opposite phenomena (i.e. necrotic or hypercellular lesions).
- Amide Proton Transfer weigthed imaging is an emerging technique that promises high diagnostic performances for assessing treatment response in brain tumors.

THE FUNDAMENTALS OF RADIONECROSIS AND PSEUDOPROGRESSION

Radiotherapy is a well established treatment option against brain primary tumors or metastases, which together account for the majority of brain tumors [1]. Stereotactic radiosurgery (SRS) is currently the most relevant therapeutic option for selected patients with brain metastasis and its indications are continuously expanding [2▪▪]. Maximum well tolerated surgical resection followed by a 6-week course of radiotherapy concurrently with temozolomide chemotherapy is the cornerstone of glioblastoma treatment [3]. Salvage re-irradiation may also be considered in some case of recurrent glioblastoma [4], although an optimal dosing regimen has not been established [5].

Unfortunately, brain radiotherapy is likely to induce chronic inflammatory reactions [6,7] and possibly result in necrotic and edematous lesions that can be extremely difficult to distinguish from tumor recurrence with both conventional and advanced MRI sequences [8,9,10▪▪,11].

Several risk factors can predispose to radio-induced brain complications. Among them, the type of systemic concurrent antitumor therapy plays an important role in enhancing radiation toxicity [12]. Notably, Immune-Checkpoint Inhibitors (ICIs), a recent target strategy against metastatic disease [2▪▪,13], are often combined with SRS [14▪] as focal irradiation can improve systemic antitumor immunity, a phenomenon typically referred as the abscopal effect [15,16]. Nevertheless, this combinatorial approach increases the risk of radiation necrosis [17], with largely unknown pathophysiological mechanisms [18]. Additionally, even in the absence of irradiation, immunotherapy agents can provoke unconventional transient immune-related phenomena that lead to misleading pseudoprogressing contrast-enhancing lesions [19].

Due to widespread use of these advanced therapeutic approaches, knowledge of these complex cutting-edge treatments is essential to properly assess treatment response and guide subsequent clinical decisions.

Definitions

There is no clear evidence nor consensus on the distinction between pseudoprogression and radionecrosis, probably because of the paucity of histopathological data, difficulties in assessing the correct histological diagnosis, given the frequent 'mixed' pattern with tumor remnants and radiation-induced tissue changes in biopsy samples [20], and the absence of large-scale, harmonized, multicenter, prospective researches.

Pseudoprogression and radionecrosis are radiologically defined by a new or enlarging area(s) in the radiation field that resolves without treatment modification. When images of radiation-induced lesions appear shortly after the end of radiotherapy (within the first 6 months for most of the studies [8,21,22], whereas others only consider the first 2 [23] or 3 months [24,25]), the term pseudoprogression is preferred, especially in the context of diffuse glioma. On the contrary, radionecrosis emerges at a later stage (from around 6 months to several years) [8,26].

Mechanism

Pathologically, no clear boundaries separate these two entities as the physiopathology of the radio-induced lesion is dynamic [27,28]. Pseudoprogression is probably an expression of early delayed brain injury and is dominated by vascular damage (i.e. vasodilation and increased capillary permeability), resulting in vasogenic edema that normally resolves spontaneously, and is often associated with transient demyelination [29]. Conversely, radionecrosis is part of late delayed brain injury and is characterized by a mixture of vascular endothelial damage and demyelination lesions, followed by neuronal death, and often does not recede [24].

Even though our understanding of the biomolecular pathways following radiotherapy is still very limited, blood vessel damage has been repeatedly recognized as one of the core step in the development of radiation toxicity [29–31], leading to hypoxia and upregulation of Hypoxia Inducible Factor-1 alpha (HIF-1α) in microglia and subsequent Vascular Endothelial Growth Factor (VEGF) induction, and several pro-inflammatory cytokines release [32]. VEGF over-expression results in leaky angiogenesis

and ultimately facilitates radio-induced necrotic lesion expansion [33–35].

Incidence

Pseudoprogression and radionecrosis are common entities in both gliomas and in brain metastases. A recent meta-analysis showed that pseudoprogression occurred in 36% (95% confidence interval, 33– 40%) high-grade glioma patients [36]. At the same time, nearly a third of SRS-treated metastases show a transient, moderate volume increase at around 6 weeks after treatments, which sometimes lasts beyond 15 months [26,37,38]. The incidence of later (after 6 months) radionecrotic lesions is less understood for both primary and secondary brain tumors, as reported incidence ranges widely from 5 to 50%, and is probably underestimated [24,34,39–41].

Risk factors

Radiotherapy toxicity is complex and depends on several parameters. Total irradiation dose [42,43], treated volume [44,45] and the dose per fraction [46] are important and obvious risk factors. In the context of diffuse gliomas, it has been suggested that MGMT promoter methylated tumors are more prone to develop pseudoprogression [47] and that temozolamide increases radiation-induced lesions in both high grade [23] and low-grade glioma [48]. Immunotherapy may raise the incidence of radionecrosis in brain metastases treated with SRS [17,19] but further studies are needed to quantify its impact [14▪,18,49]. All in all, the intertangled network of these heterogeneous predisposing factors is largely unknown, and it is impossible to predict individual sensitivity to radiation toxicity. Large, multivariate analysis are certainly needed, and they should include an extensive panel on molecular tumor characteristics and all different types of concurrent or adjuvant antitumor agents.

Clinical implications

Radiation-induced toxicity is usually asymptomatic or paucisymptomatic [44]. When radiation necrosis is clinically meaningful, it is commonly treated with high-dose steroids or with surgical debulking [50,51]. Given the role of VEGF on the radiation-induced progressing lesion [35,52], it is not surprising that bevacizumab, an anti-VEGF monoclonal antibody, is also an effective treatment for symptomatic steroid-resistant radiation necrosis of both primary [53] and secondary tumors [54,55▪,56] and that it may help reducing steroid dosage [57]. Hyperbaric oxygen [58], laser interstitial thermal therapy [50] and anti-TNF antibodies [59,60] are other treatment options but have only been investigated in preliminary reports.

In the most frequent scenario, the clinical challenge is not simply to treat radiation-induced lesions but firstly to diagnose it correctly. Resolving this clinical problem is crucial as it permits to avoid premature cessation of effective treatments or delays in withdrawal of ineffective treatments. To date, no validated single MRI-based imaging metric can differentiate between treatment response and tumor recurrence after radiation therapy. Therefore, a multimodality approach is almost always required, although sometimes still insufficient because of intrinsic limitations of the available MRI sequences, as furtherly discussed.

CURRENT MRI IMAGING IN POSTTREATMENT TUMOR EVALUATION

The Response Assessment in Neuro-Oncology (RANO) working group has provided consensus response criteria for high-grade [61] and low-grade [62] gliomas, and for brain metastases with the commendable purposes of accuracy and reproducibility between different institutions. At present, however, it is extremely difficult to combine these two characteristics in posttherapeutic assessment of brain tumors as accuracy requires advanced multimodal imaging protocols that are extremely difficult to standardize and validate in multicenter studies. On the other hand, reproducibility can be achieved with conventional imaging but it is often far from being accurate. At present, on the urge of interpretation of clinical trials, reproducibility has been preferred and RANO criteria are based on conventional MRI sequences [63]. To overcome inherent limitation of RANO criteria on the evaluation of pseudoprogressing lesions during ICIs trials, immunotherapy response assessment for neuro-oncology (iRANO) criteria [64] have been developed but they are still based on morphological imaging features, and therefore, lead to delayed diagnosis.

Conventional sequences

Visual inspection of T_1-weighted (T_1w), T_2-weighted (T_2w), and fluid-attenuated inversion recovery (FLAIR) sequences is essential for detecting fine anatomical details but it is useless in the metabolic discrimination of space-occupying lesion. Morphological imaging after contrast agent injection detects blood–brain barrier leakage, which is present in both radiation-induced inflammation and in neoplastic lesion [8]. Early studies explored the value of

T_2w and T_1w postcontrast imaging in differentiating tumor recurrence from radiation necrosis in brain metastases treated with SRS. Evaluation of the spatial concordance between the boundaries of the lesion on T_2w and T_1w postcontrast imaging show a T1/T2 match (in favor of tumor recurrence) or T1/T2 mismatch (in favor of radionecrosis) [65]. Quantitative determination of lesion quotient, defined as the area of a hypointense nodule on T_2w divided by its area on contrast-enhanced T_1w, suggested to show different results in radionecrosis (lesion quotient less than 0.3) and in recurrent metastasis (lesion quotient greater than 0.6) [66]. These qualitative and quantitative signs were not confirmed in further studies [67,68].

Type of contrast uptake has also been investigated, and a 'cut-green pepper', a 'soapbubbles' or a 'gruyere' cheese contrast enhancement appearance has been related to radionecrosis [69,70] but the subjective evaluation of these signs limits their reproducibility [9].

Overall, conventional sequence evaluation does not distinguish between tumor and posttherapeutic lesion at an early stage [71], whereas in the later stage, the tumor progresses while the posttherapeutic lesion remains stable, shrink or disappear.

Diffusion-weighted imaging

Diffusion-weighted imaging and its various extensions (diffusion tensor imaging, diffusion kurtosis imaging, neurite orientation dispersion and density imaging, diffusional and constrained diffusional variance decomposition) can provide important complementary information on tissue microstructure in treatment-naive patients [72–76]. Conversely, after radiotherapy, the evaluation of diffusion-derived changes must be interpreted with caution as studies on this topic are contradictory [77,78] and similar diffusion water molecules metric can reflect opposite phenomena (i.e. diffusion restriction because of hypercellularity or postradiotherapy coagulative necrosis) [72,79]. An example of diffusion restriction in a pathologically proved radionecrosis is shown in Fig. 1. Detection of restricted diffusion foci in irradiated tumor successively treated with Bevacizumab is a well known form of therapy-induced necrosis [80,81]. Radiologist and clinicians should be aware of this entity and avoid misdiagnosis with stroke or tumor progression.

Intravoxel Coherent Motion Imaging, a novel diffusion technique that produces simultaneous diffusion and perfusion maps, can have a potential role in identifying radiation-induced changes in gliomas and brain metastases treated with SRS, as a pilot works suggest [82].

Susceptibility-weighted imaging

Several paramagnetic and diamagnetic sources of signal, such as deoxygenated hemoglobin, tissue calcifications or iron deposits can alter magnetic susceptibility and thus lead to susceptibility-weighted imaging (SWI) changes. They can be present in brain metastases, especially of melanoma [83▪], and in glioma [84]. In this latter group, the degree of intratumoral susceptibility signal intensity (ITSS) was shown to be positively correlated with glioma grade and higher perfusion values [85]. After radiotherapy, a marked increase of SWI signal changes within the radiation field is often observed, traducing blood vessel injury and radiotherapy-related remnants [79,86]. Measuring the proportion of hemorrhage shown in SWI lowers false-positive rate in the differentiation of recurrence from radionecrosis-based simply on perfusion measurements [87] and increases overall survival prediction [87].

R_2^* coefficient is also sensitive to hemorrhage and calcifications, and it can be measured within a specific region of interest by fitting signal decay through multiechoes gradient echo sequences. A pilot study in glioblastoma patients showed that this coefficient, also referred as apparent transverse relaxation, shows lower value in pseudoprogressing compared with progressing contrast –enhancing lesions [88]. Preclinical data suggest that R_2^* coefficient might even predict radionecrosis 10 weeks before morphological changes [89].

Brain perfusion

Brain MRI tumor perfusion measures can be acquired through dynamic susceptibility contrast (DSC), dynamic contrast-enhanced (DCE), or arterial spin labelling (ASL) techniques. Relative Cerebral Blood Volume (rCBV) value, a semi-quantitative vascularity measure derived from DSC perfusion, is the most used advanced MRI indicator in posttreatment tumor assessment [90–93], with a cutoff of the contralateral white matter Region of Interest (ROI) usually ranging above 1.5–2 for tumor lesions [94–96]. Elevated rCBV is a marker of increased microvascular density and often reflects tumor aggressiveness, correlating with glioma grade [97] and survival [98] (except for oligodendrogliomas [99]). The increase in rCBV compared with baseline after antitumor treatment predicts a worse outcome [100,101] and seems more accurate in survival prediction than histopathologic grade in glioma [102].

In SRS-treated metastasis, the percentage signal-intensity recovery (PSR) towards baseline, an indicator of capillary permeability, appears to be a better prognostic indicator of metastatic tumor

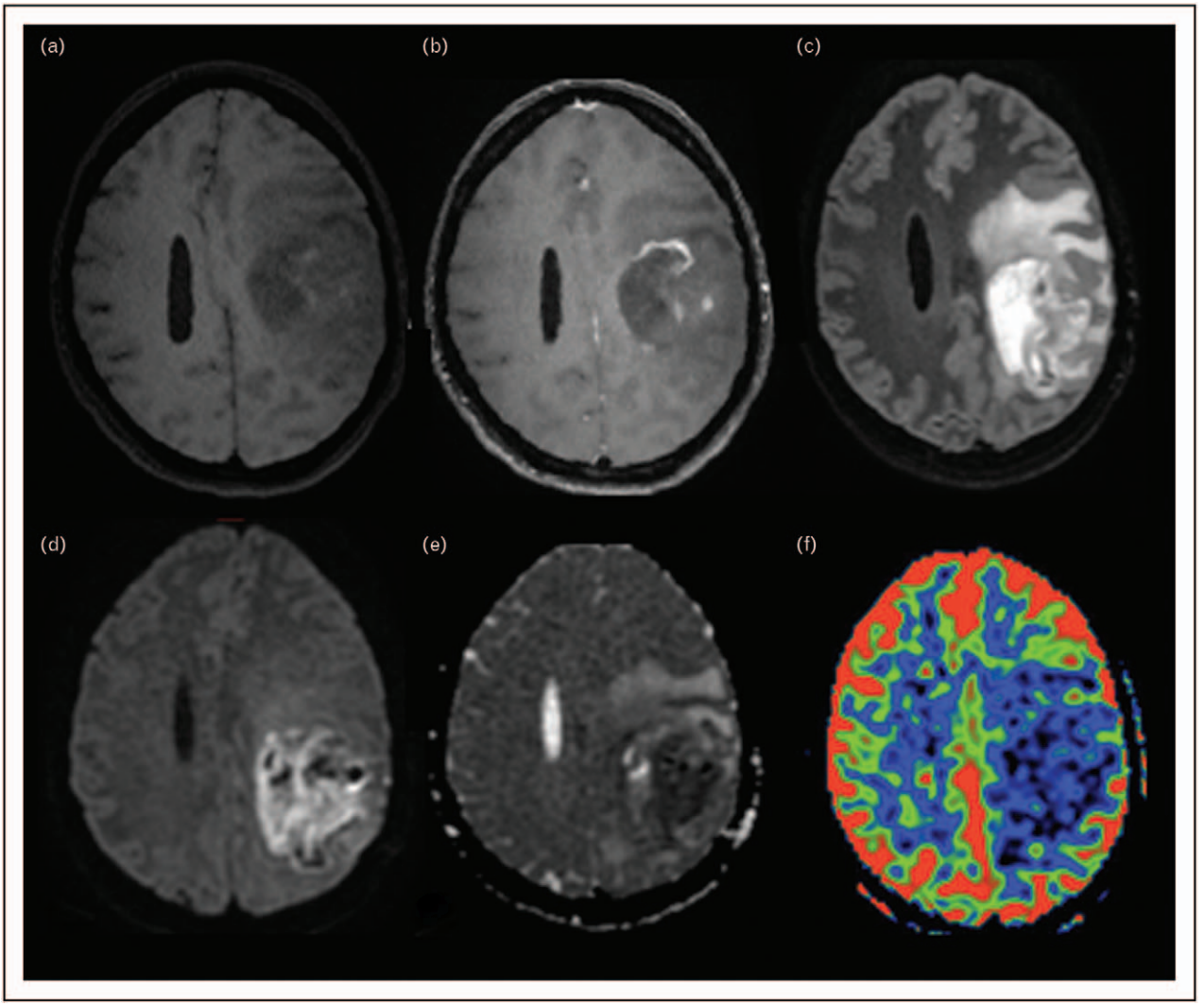

FIGURE 1. Pathologically proven radionecrosis in a 45 years old woman with anaplastic pleomorphic xanthoastrocytoma treated with Stupp protocol (radiotherapy and concurrent chemotherapy with temozolomide). Axial 3D T_1w spin echo before (a) and after (b) gadolinium injection showed a contrast-enhancing intra-axial frontal lesion, with some hemorrhagic remnants that were spontaneously bright on T_1w. This lesion was surrounded by a large nonenhancing FLAIR hyperintensity, visible on axial 3D FLAIR (c) and it was characterized by a strong diffusion restriction (d: axial diffusion with b100 value, e: ADC cartography). No hyperperfusion was seen [f: axial arterial spin labelling (ASL) perfusion]. This radio-induced lesion developed 2 months after the end of radiotherapy. ADC, apparent diffusion coefficient.

progression than rCBV as radiation-induced lesions show a higher PSR than do recurrent tumors [103].

Unfortunately, because of the difficulty in controlling several technical acquisition and postprocessing variables, there are considerable interinstitutional and even intrainstitutional variations in DSC-derived measurements [104]. This variability severely limits reproducibility and hampers the implementation of DSC perfusion in the routine assessment of treatment response (e.g. current RANO criteria) [105].

DCE-MRI data enable the evaluation of several pharmacokinetics parameters. The most investigated is the volume transfer coefficient (K^{trans}) that reflects the tumor vascular permeability and is higher in radiation necrosis than in tumor progression [106–109]. In brain metastatic disease, DCE technique appears to have better diagnostic accuracy than DCS perfusion in the differential diagnosis between radiation necrosis and tumor recurrence [110]. In contrast, high-grade glioma DSC-derived blood volume measures seem more accurate than DCE-derived permeability measures in the same distinction [111,112].

ASL is a contrast-free perfusion technique obtained through magnetically labeled blood protons. ASL imaging is starting to be studied in high-

grade gliomas [113], especially in posttherapeutic settings, where it showed no need of leakage-correction algorithms, fewer susceptibility artifacts than DSC perfusion [114] but contrasting accuracy results. To date, no studies have been published on the ASL performance in brain metastasis posttreatment evaluation.

Spectroscopy

Magnetic resonance spectroscopy (MRS) provides insight into metabolic tissue features by noninvasively detecting solute protons in water. Concentration of choline-containing compound metabolites, markers of cell membrane turnover, is highly increased in tumor progression [115], whereas lipids and lactates have been shown to dominate in posttreatment disease, suggesting cellular necrosis [116]. Several metabolite ratios have been proposed to diagnose radionecrotic lesion (summarized in previous reviews [117–119]), and Cho/NAA and Cho/Cr ratios seem to be the best discriminators [120] but none of them have been validated in multicenter studies. When compared with perfusion, MRS showed inferior discriminating abilities [121]. However, the combination of MRS and perfusion imaging increases diagnostic accuracy [111,122], hence with sensitivity and specificity values that still prevent replacing invasive biopsy sampling or serial imaging confirmation.

D-2-hydroxyglutarate (2HG) MRS [123] is an umbrella term that refers to MRS techniques that can measure 2HG oncometabolite [124] in IDH-mutant diffuse gliomas. Preliminary longitudinal 2HG MRS evaluations have shown that this biomarker decreases after antitumor treatments [125] and possibly increases in tumor recurrence [126], thus this novel noninvasive technique could also aid in IDH-mutant glioma posttreatment assessment.

Texture analysis and radiomics

The term ‘texture analysis’ encompasses different computational methods that are used to quantify the spatial arrangement of image signal intensities. After ROI definition and preprocessing, several features, imperceptibles to the human eye, are extracted, selected and finally classified [127]. The complementary information provided by this noninvasive, objective and possibly fully automatic approach is clearly attractive but lack of standardization and overfitting issues are still major constraints [128,129]. When these multiple parameters are used to predict clinical and biological variables, this multistep approach is referred to as ‘radiomics’ [130].

MR texture analysis and radiomics have been conducted mainly with conventional sequences, with already interesting results, especially in the evaluation of tumor shape features and surface irregularities in the diagnosis of glioblastoma versus pseudoprogression [131]. Adding complementary advanced sequences to this complex evaluation indeed promises to achieve higher diagnostic performances [132,133▪▪].

CHEMICAL EXCHANGE SATURATION TRANSFER IMAGING: A NEW TOOL ON MRI ARSENAL

Chemical exchange saturation transfer (CEST) is a molecular imaging technique recently available on 3 Tesla MRI scanners [134,135] that detects low-concentration solute molecules with exchangeable hydrogen protons. By applying a radiofrequency pulse at their resonance frequencies, the chemical species of interest – such as amide (NH), amine (NH2) or hydroxyl group (OH) – reach a saturation state and their labile excited hydrogen protons are exchanged with the nonexcited hydrogen protons of solvent water. If this process is repeated continuously for a few seconds of RF irradiation, saturation builds up, which decreases water signal, thus indirectly reflecting the concentration of the targeted species with amplified detection. Their detectability is, for example, amplified by a factor of 100, if this exchange takes places 100 times [136].

To extract the CEST signal of interest, multiple samples are acquired around the frequency of water and molecules of interest to correct field inhomogeneities [137,138], for denoising purposes [139], and for averaging of the sampled values to increase the signal-to-noise ratio [140]. This set of sampled volumes (normalized for an unsaturated volume) is called the Z-Spectrum [136].

The most marked clinical distinction for this molecular technique is whether the CEST agent is endogenous (and therefore, is already found in the human body, such as the amide and amine groups from peptides and proteins [141]) or exogenous (and therefore, needs to be administered, such as glucose-based agents [142] or Iopamidol [143]).

Amide CEST imaging, also known as APT, has been shown to provide more stable and sensitive detection compared with other CEST agent on clinical 3 Tesla scanners, and therefore is, to date, the most used CEST technique, in and out of the neurological field [144]. In neuro-oncology, an increase in APT-weighted (APTw) signal intensity is observed in tumor tissues, because of elevated concentration of intracellular mobile proteins and peptides, and consequent increase of protein backbone amides.

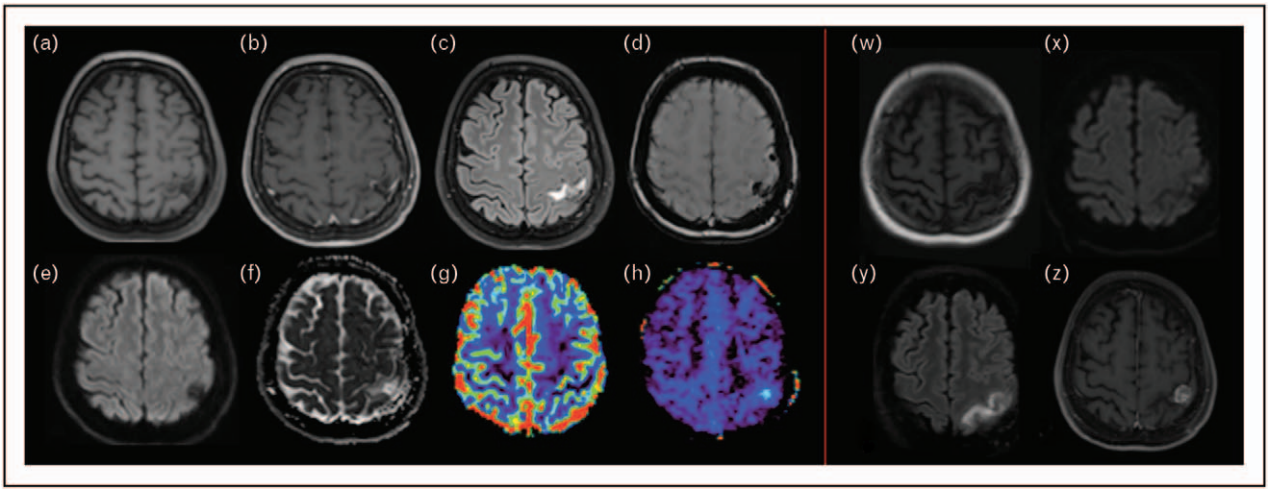

FIGURE 2. Biopsy-proven tumor progression early detected by Amide Proton Transfer and not by conventional nor perfusion MRI. A 54-year-old woman with a single brain metastases of a breast cancer was treated with surgical resection and stereotactic radiosurgery (SRS) to the surgical cavity. Nine months after SRS, a postrolandic lesion appeared, visible on noncontrast 3D T_1w spin echo (a) and showing a linear contrast-enhancement (b), and a FLAIR hyperintensity on axial 3D FLAIR sequence (c). Axial SWI (d) showed several hemosiderin remnants, axial diffusion with b100 value (e) and ADC cartography (f) showed no diffusion restriction, dynamic susceptibility contrast (DSC) perfusion (g) no neoangiogenesis. Therefore, conventional and advanced imaging suggested a radio-induced lesion. In addition, amide signal increased intensity on fluid-suppressed [150] APTw imaging (h) suspected tumor progression, and this was confirmed by a surgical resection done shorty after a 3-month MRI follow-up (w: 3D T_1w spin echo without contrast injection, x: axial diffusion with b1000 value, y: axial 3D FLAIR, z: axial 3D T1 spin echo with contrast injection). Olea Sphere 3.0 software (Olea Medical, La Ciotat, France) was used to compute APTw and perfusion maps. APT_w, Amide Proton Transfer-weighted; ADC, apparent diffusion coefficient; SWI, susceptibility-weighted imaging.

APTw imaging has demonstrated promising results in glioma grading [141,145,146], in the identification of higher cellularity and proliferation area in heterogeneous diffuse glioma [147], as in IDH status and 1p/19q co-deletion prediction [148–151].

Another major potential application of APTw imaging is the assessment of response to treatment, with the hypothesis that tumor hypercellularity leads to an increase in APTw signal intensity compared with lower cellular density of therapeutic related changes. In 2011, a first preclinical study showed a significant decrease in APTw signal intensity in the radionecrotic lesions compared with gliomas [152]. Shortly thereafter, another preclinical work showed that APTw values decrease more rapidly than diffusion and ASL perfusion values, suggesting that Amide CEST could prompt early response information [153]. The former group then conducted a first clinical radiohistopathological validation in glioma patients and found positive significant correlations between APTw signal intensity and both cellularity and proliferation index [154], therefore, suggesting that APTw values are a marker of active glioma in posttreatment settings. These results are in line with other studies that have been conducted in diffuse gliomas, especially in context of the antiangiogenic therapy [155] and in the distinction between progressing and pseudoprogressing lesion [149]. Interestingly, the changes in APTw signal intensity was also seen to spatially overlap FET-PET data for both contrast-enhancing and noncontrast-enhancing glioma lesions [156], which is easily explained as biological processes behind this different imaging modalities are similar.

Concerning brain metastases, previous study reported that not only the CEST signal from amide groups but also from the Nuclear Overhauser Enhancement (NOE) effects, a protein un-folding biomarker [157] that can be derived through CEST imaging fitting [138,158], was able to distinguish radiation necrosis from tumor progression, and NOE signal intensity provided the best separation of these two conditions [158].

Advances in CEST imaging are increasing the ability to extract both individual APT and NOE biomarkers in clinical routine [134,159] without the contamination of magnetization transfer effect coming from semisolid macromolecules [136].

Figure 2 illustrates an example of biopsy-proven tumor progression that was early detected by APTw imaging and neither by conventional nor perfusion MRI, whereas Fig. 3 displays a radiation-induced lesion that regressed at 6-month follow-up.

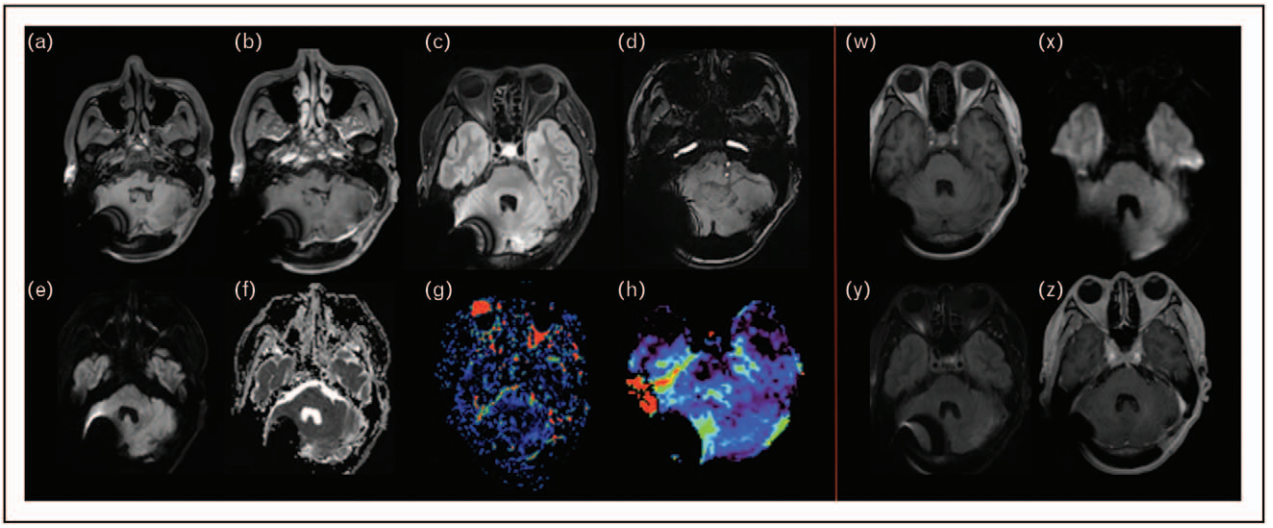

FIGURE 3. Radiation-induced contrast-enhancing lesion that regressed at 6-month follow-up. A 46-year-old patient with a single brain metastases of a lung cancer was treated with surgical resection and stereotactic radiosurgery (SRS) to the surgical cavity. Four months after SRS, an irregular, nonnodular contrast enhancing lesion appeared (a: noncontrast 3D T_1w spin echo, b: postcontrast 3D T_1w spin echo, c: axial 3D FLAIR) with several hemosiderin remnants visible on axial SWI (d). The lesion showed neither diffusion restriction (e: axial diffusion with b100 value, f: ADC map) nor neoangiogenesis on axial DSC perfusion (g) nor amide signal increased intensity on fluid-suppressed APT-weighted imaging (h). Therefore, a radio-induced lesion was suspected. This diagnosis was confirmed at a 6-month MRI follow-up, where the contrast enhancement disappeared (w: 3D T_1w spin echo without contrast injection, x: axial diffusion with b1000 value, y: axial 3D FLAIR, z: axial 3D T1 spin echo with contrast injection). Olea Sphere 3.0 software (Olea Medical, La Ciotat, France) was used to compute the APTw map. APT_w, Amide Proton Transfer-weighted; ADC, apparent diffusion coefficient; SWI, susceptibility-weighted imaging.

CONCLUSION

Radionecrosis and pseudoprogression are common phenomena that urge precise imaging diagnosis to provide optimal early patient care. Shortcomings of conventional MRI are well known, whereas the added value of complementary advanced imaging sequences, especially perfusion, needs to be accurately established, as inherent limitations have been reported for each sequence. In this evolving scenario, APT-CEST metrics offer new problem-solving tools that expand MRI armamentarium for assessing treatment response. A multimodal machine-learning analysis that includes the best performing perfusion technique with validated molecular information provided by CEST imaging promises highly accurate personalized patient care of each individual brain lesion.

Acknowledgements

We acknowledge the help of Stéphane Lehéricy (Department of Neuroradiology, La Pitié Salpêtrière - Charles Foix Hospital, Paris, France), Julian Jacob (Department of Radiation Oncology, La Pitié Salpêtrière - Charles Foix Hospital, Paris, France) and Malgorzata Marjanska (Center for Magnetic Resonance Research, Department of Radiology, Minneapolis, Minnesota, United States) for their critical revision of the article. We thank Christos Papageorgakis (Department of Research & Innovation, Olea Medical, La Ciotat, France) for MR acquisition processing support.

Financial support and sponsorship

None.

Conflicts of interest

L.N. has no financial disclosure. S.C. is currently an employee at Olea Medical (Research & Innovation Team Leader – Molecular Imaging Project Manager).

REFERENCES AND RECOMMENDED READING

Papers of particular interest, published within the annual period of review, have been highlighted as:

- ■ of special interest
- ■■ of outstanding interest

1. Louis DN, Perry A, Reifenberger G, *et al.* The 2016 World Health Organization Classification of Tumors of the Central Nervous System: a summary. Acta Neuropathol (Berl) 2016; 131:803–820.
2. ■■ Suh JH, Kotecha R, Chao ST, *et al.* Current approaches to the management of brain metastases. Nat Rev Clin Oncol 2020; 17:279–299.

This article contains an exhaustive description on the current treatment and management of patients with brain metastases.

3. Stupp R, Mason WP, van den Bent MJ, *et al.* Radiotherapy plus concomitant and adjuvant temozolomide for glioblastoma. N Engl J Med 2005; 352:987–996.

4. Shah JL, Li G, Shaffer JL, *et al.* Stereotactic radiosurgery and hypofractionated radiotherapy for glioblastoma. Neurosurgery 2018; 82:24–34.
5. Kazmi F, Soon YY, Leong YH, *et al.* Re-irradiation for recurrent glioblastoma (GBM): a systematic review and meta-analysis. J Neurooncol 2019; 142:79–90.
6. Soussain C, Ricard D, Fike JR, *et al.* CNS complications of radiotherapy and chemotherapy. The Lancet 2009; 374:1639–1651.
7. De Ruysscher D, Niedermann G, Burnet NG, *et al.* Radiotherapy toxicity. Nat Rev Dis Primer 2019; 5:13.
8. Ellingson BM, Chung C, Pope WB, *et al.* Pseudoprogression, radionecrosis, inflammation or true tumor progression? challenges associated with glioblastoma response assessment in an evolving therapeutic landscape. J Neurooncol 2017; 134:495–504.
9. Thust SC, van den Bent MJ, Smits M. Pseudoprogression of brain tumors: pseudoprogression of brain tumors. J Magn Reson Imaging 2018; 48:571–589.
10. Katsura M, Sato J, Akahane M, *et al.* Recognizing radiation-induced changes
■■ in the central nervous system: where to look and what to look for. RadioGraphics 2021; 41:224–248.

This very clear and didactic review summarizes the vast spectrum of radiation-induced lesion of the central nervous system.

11. Ly KI, Gerstner ER. The role of advanced brain tumor imaging in the care of patients with central nervous system malignancies. Curr Treat Options Oncol 2018; 19:40.
12. Ruben JD, Dally M, Bailey M, *et al.* Cerebral radiation necrosis: Incidence, outcomes, and risk factors with emphasis on radiation parameters and chemotherapy. Int J Radiat Oncol 2006; 65:499–508.
13. Valiente M, Ahluwalia MS, Boire A, *et al.* The evolving landscape of brain metastasis. Trends Cancer 2018; 4:176–196.
14. Pin Y, Paix A, Todeschi J, *et al.* Brain metastasis formation and irradiation by
■ stereotactic radiation therapy combined with immunotherapy: a systematic review. Crit Rev Oncol Hematol 2020; 149:102923.

This review covers the current state-of-the-art on brain metastases treated with irradiation and immunotherapy, an emerging therapeutic approach that seems to increase radionecrotic lesions.

15. Ashrafizadeh M, Farhood B, Eleojo Musa A, *et al.* Abscopal effect in radioimmunotherapy. Int Immunopharmacol 2020; 85:106663.
16. Ngwa W, Irabor OC, Schoenfeld JD, *et al.* Using immunotherapy to boost the abscopal effect. Nat Rev Cancer 2018; 18:313–322.
17. Colaco RJ, Martin P, Kluger HM, *et al.* Does immunotherapy increase the rate of radiation necrosis after radiosurgical treatment of brain metastases? J Neurosurg 2016; 125:17–23.
18. Hwang WL, Pike LRG, Royce TJ, *et al.* Safety of combining radiotherapy with immune-checkpoint inhibition. Nat Rev Clin Oncol 2018; 15:477–494.
19. Wang Q, Gao J, Wu X. Pseudoprogression and hyperprogression after checkpoint blockade. Int Immunopharmacol 2018; 58:125–135.
20. Melguizo-Gavilanes I, Bruner JM, Guha-Thakurta N, *et al.* Characterization of pseudoprogression in patients with glioblastoma: is histology the gold standard? J Neurooncol 2015; 123:141–150.
21. de Wit MCY, de Bruin HG, Eijkenboom W, *et al.* Immediate postradiotherapy changes in malignant glioma can mimic tumor progression. Neurology 2004; 63:535–537.
22. Pope WB. Brain metastases: neuroimaging. Handb Clin Neurol 2018; 149:89–112.
23. Taal W, Brandsma D, de Bruin HG, *et al.* The incidence of pseudo-progression in a cohort of malignant glioma patients treated with chemo-radiation with temozolomide. J Clin Oncol 2007; 25(18 Suppl):2009–12009.
24. Brandsma D, Stalpers L, Taal W, *et al.* Clinical features, mechanisms, and management of pseudoprogression in malignant gliomas. Lancet Oncol 2008; 9:453–461.
25. Rowe LS, Butman JA, Mackey M, *et al.* Differentiating pseudoprogression from true progression: analysis of radiographic, biologic, and clinical clues in GBM. J Neurooncol 2018; 139:145–152.
26. Le Rhun E, Dhermain F, Vogin G, *et al.* Radionecrosis after stereotactic radiotherapy for brain metastases. Expert Rev Neurother 2016; 16:903–914.
27. Schaue D, Micewicz ED, Ratikan JA, *et al.* Radiation and inflammation. Semin Radiat Oncol 2015; 25:4–10.
28. Tofilon PJ, Fike JR. The radioresponse of the central nervous system: a dynamic process. Radiat Res 2000; 153:357–370.
29. Wong CS. Mechanisms of radiation injury to the central nervous system: implications for neuroprotection. Mol Interv 2004; 4:273–284.
30. Miyatake S-I, Nonoguchi N, Furuse M, *et al.* Pathophysiology, diagnosis, and treatment of radiation necrosis in the brain. Neurol Med Chir (Tokyo) 2015; 55:50–59.
31. Burger PC, Mahley MS, Dudka L, Vogel FS. The morphologic effects of radiation administered therapeutically for intracranial gliomas: a postmortem study of 25 cases. Cancer 1979; 44:1256–1272.
32. Fink J, Born D, Chamberlain MC. Radiation necrosis: relevance with respect to treatment of primary and secondary brain tumors. Curr Neurol Neurosci Rep 2012; 12:276–285.
33. Yoshii Y. Pathological review of late cerebral radionecrosis. Brain Tumor Pathol 2008; 25:51–58.
34. Furuse M, Nonoguchi N, Kawabata S, *et al.* Delayed brain radiation necrosis: pathological review and new molecular targets for treatment. Med Mol Morphol 2015; 48:183–190.
35. Zhuang H, Shi S, Yuan Z, Chang JY. Bevacizumab treatment for radiation brain necrosis: mechanism, efficacy and issues. Mol Cancer 2019; 18:21.
36. Abbasi AW, Westerlaan HE, Holtman GA, *et al.* Incidence of tumour progression and pseudoprogression in high-grade gliomas: a systematic review and meta-analysis. Clin Neuroradiol 2018; 28:401–411.
37. Patel TR, McHugh BJ, Bi WL, *et al.* A comprehensive review of MR imaging changes following radiosurgery to 500 brain metastases. Am J Neuroradiol 2011; 32:1885–1892.
38. Minniti G, Clarke E, Lanzetta G, *et al.* Stereotactic radiosurgery for brain metastases: analysis of outcome and risk of brain radionecrosis. Radiat Oncol Lond Engl 2011; 6:48.
39. Emami B, Lyman J, Brown A, *et al.* Tolerance of normal tissue to therapeutic irradiation. Int J Radiat Oncol 1991; 21:109–122.
40. Narloch JL, Farber SH, Sammons S, *et al.* Biopsy of enlarging lesions after stereotactic radiosurgery for brain metastases frequently reveals radiation necrosis. Neuro-Oncol 2017; 19:1391–1397.
41. Fujimoto D, von Eyben R, Gibbs IC, *et al.* Imaging changes over 18 months following stereotactic radiosurgery for brain metastases: both late radiation necrosis and tumor progression can occur. J Neurooncol 2018; 136:207–212.
42. Donovan EK, Parpia S, Greenspoon JN. Incidence of radionecrosis in single-fraction radiosurgery compared with fractionated radiotherapy in the treatment of brain metastasis. Curr Oncol Tor Ont 2019; 26: e328–e333.
43. Marks JE, Bag̀lan RJ, Prassad SC, Blank WF. Cerebral radionecrosis: incidence and risk in relation to dose, time, fractionation and volume. Int J Radiat Oncol 1981; 7:243–252.
44. Korytko T, Radivoyevitch T, Colussi V, *et al.* 12 Gy gamma knife radiosurgical volume is a predictor for radiation necrosis in non-AVM intracranial tumors. Int J Radiat Oncol 2006; 64:419–424.
45. Blonigen BJ, Steinmetz RD, Levin L, *et al.* Irradiated volume as a predictor of brain radionecrosis after linear accelerator stereotactic radiosurgery. Int J Radiat Oncol 2010; 77:996–1001.
46. Lee AWM, Kwong DLW, Leung S-F, *et al.* Factors affecting risk of symptomatic temporal lobe necrosis: significance of fractional dose and treatment time. Int J Radiat Oncol 2002; 53:75–85.
47. Brandes AA, Franceschi E, Tosoni A, *et al. MGMT* promoter methylation status can predict the incidence and outcome of pseudoprogression after concomitant radiochemotherapy in newly diagnosed glioblastoma patients. J Clin Oncol 2008; 26:2192–2197.
48. Dworkin M, Mehan W, Niemierko A, *et al.* Increase of pseudoprogression and other treatment related effects in low-grade glioma patients treated with proton radiation and temozolomide. J Neurooncol 2019; 142:69–77.
49. Andring L, Squires B, Seymour Z, *et al.* Radionecrosis (RN) in patients with brain metastases treated with stereotactic radiosurgery (SRS) and immunotherapy. Int J Neurosci 2021; 1–8.
50. Rahmathulla G, Marko NF, Weil RJ. Cerebral radiation necrosis: a review of the pathobiology, diagnosis and management considerations. J Clin Neurosci 2013; 20:485–502.
51. Stockham AL, Ahluwalia M, Reddy CA, *et al.* Results of a questionnaire regarding practice patterns for the diagnosis and treatment of intracranial radiation necrosis after SRS. J Neurooncol 2013; 115:469–475.
52. Delishaj D, Ursino S, Pasqualetti F, *et al.* Bevacizumab for the treatment of radiation-induced cerebral necrosis: a systematic review of the literature. J Clin Med Res 2017; 9:273–280.
53. Fleischmann DF, Jenn J, Corradini S, *et al.* Bevacizumab reduces toxicity of reirradiation in recurrent high-grade glioma. Radiother Oncol 2019; 138:99–105.
54. Tripathi M, Ahuja C, Mukherjee K, *et al.* The safety and efficacy of bevacizumab for radiosurgery - induced steroid - resistant brain edema; not the last part in the Ship of Theseus. Neurol India 2019; 67:1292–1302.
55. Khan M, Zhao Z, Arooj S, Liao G. Bevacizumab for radiation necrosis
■ following radiotherapy of brain metastatic disease: a systematic review and meta-analysis. BMC Cancer 2021; 21:167.

This review summarizes the current knowledge on bevacizumab-induced radionecrosis, a common emerging clinicoradiological entity.

56. Boothe D, Young R, Yamada Y, *et al.* Bevacizumab as a treatment for radiation necrosis of brain metastases post stereotactic radiosurgery. Neuro-Oncol 2013; 15:1257–1263.
57. Banks PD, Lasocki A, Lau PKH, *et al.* Bevacizumab as a steroid-sparing agent during immunotherapy for melanoma brain metastases: A case series. Health Sci Rep 2019; 2:e115.
58. Co J, De Moraes MV, Katznelson R, *et al.* Hyperbaric oxygen for radiation necrosis of the brain. Can J Neurol Sci J Can Sci Neurol 2020; 47:92–99.
59. Ansari R, Gaber MW, Wang B, *et al.* Anti-TNFA (TNF-α) treatment abrogates radiation-induced changes in vascular density and tissue oxygenation. Radiat Res 2007; 167:80–86.
60. Wilson CM, Gaber MW, Sabek OM, *et al.* Radiation-induced astrogliosis and blood-brain barrier damage can be abrogated using anti-TNF treatment. Int J Radiat Oncol 2009; 74:934–941.

61. Wen PY, Macdonald DR, Reardon DA, *et al.* Updated response assessment criteria for high-grade gliomas: response assessment in Neuro-Oncology Working Group. J Clin Oncol 2010; 28:1963–1972.

62. van den Bent M, Wefel J, Schiff D, *et al.* Response assessment in neuro-oncology (a report of the RANO group): assessment of outcome in trials of diffuse low-grade gliomas. Lancet Oncol 2011; 12:583–593.

63. Leao DJ, Craig PG, Godoy LF, *et al.* Response assessment in neuro-oncology criteria for gliomas: practical approach using conventional and advanced techniques. Am J Neuroradiol 2020; 41:10–20.

64. Okada H, Weller M, Huang R, *et al.* Immunotherapy response assessment in neuro-oncology: a report of the RANO working group. Lancet Oncol 2015; 16:e534–e542.

65. Kano H, Kondziolka D, Lobato-Polo J, *et al.* T1/T2 matching to differentiate tumor growth from radiation effects after stereotactic radiosurgery. Neurosurgery 2010; 66:486–492.

66. Dequesada IM, Quisling RG, Yachnis A, Friedman WA. Can standard magnetic resonance imaging reliably distinguish recurrent tumor from radiation necrosis after radiosurgery for brain metastases? A radiographic-pathological study. Neurosurgery 2008; 63:898–904.

67. Stockham AL, Tievsky AL, Koyfman SA, *et al.* Conventional MRI does not reliably distinguish radiation necrosis from tumor recurrence after stereotactic radiosurgery. J Neurooncol 2012; 109:149–158.

68. Leeman JE, Clump DA, Flickinger JC, *et al.* Extent of perilesional edema differentiates radionecrosis from tumor recurrence following stereotactic radiosurgery for brain metastases. Neuro-Oncol 2013; 15:1732–1738.

69. Kumar AJ, Leeds NE, Fuller GN, *et al.* Malignant gliomas: MR imaging spectrum of radiation therapy- and chemotherapy-induced necrosis of the brain after treatment. Radiology 2000; 217:377–384.

70. Mullins ME, Barest GD, Schaefer PW, *et al.* Radiation necrosis versus glioma recurrence: conventional MR imaging clues to diagnosis. AJNR Am J Neuroradiol 2005; 26:1967–1972.

71. van Dijken BRJ, van Laar PJ, Holtman GA, van der Hoorn A. Diagnostic accuracy of magnetic resonance imaging techniques for treatment response evaluation in patients with high-grade glioma, a systematic review and meta-analysis. Eur Radiol 2017; 27:4129–4144.

72. Hein PA, Eskey CJ, Dunn JF, Hug EB. Diffusion-weighted imaging in the follow-up of treated high-grade gliomas: tumor recurrence versus radiation injury. AJNR Am J Neuroradiol 2004; 25:201–209.

73. Masjoodi S, Hashemi H, Oghabian MA, Sharifi G. Differentiation of edematous, tumoral and normal areas of brain using diffusion tensor and neurite orientation dispersion and density imaging. J Biomed Phys Eng 2018; 8:251–260.

74. Wen Q, Kelley DAC, Banerjee S, *et al.* Clinically feasible NODDI characterization of glioma using multiband EPI at 7 T. NeuroImage Clin 2015; 9:291–299.

75. Jiang R, Jiang J, Zhao L, *et al.* Diffusion kurtosis imaging can efficiently assess the glioma grade and cellular proliferation. Oncotarget 2015; 6:42380–42393.

76. Szczepankiewicz F, van Westen D, Englund E, *et al.* The link between diffusion MRI and tumor heterogeneity: mapping cell eccentricity and density by diffusional variance decomposition (DIVIDE). NeuroImage 2016; 142:522–532.

77. Chen Z, Zu J, Li L, *et al.* Assessment of stereotactic radiosurgery treatment response for brain metastases using MRI based diffusion index. Eur J Radiol Open 2017; 4:84–88.

78. Sundgren PC, Fan X, Weybright P, *et al.* Differentiation of recurrent brain tumor versus radiation injury using diffusion tensor imaging in patients with new contrast-enhancing lesions. Magn Reson Imaging 2006; 24:1131–1142.

79. Zeng Q-S, Li C-F, Liu H, *et al.* Distinction between recurrent glioma and radiation injury using magnetic resonance spectroscopy in combination with diffusion-weighted imaging. Int J Radiat Oncol 2007; 68:151–158.

80. Mong S, Ellingson BM, Nghiemphu PL, *et al.* Persistent diffusion-restricted lesions in bevacizumab-treated malignant gliomas are associated with improved survival compared with matched controls. Am J Neuroradiol 2012; 33:1763–1770.

81. Nguyen HS, Milbach N, Hurrell SL, *et al.* Progressing bevacizumab-induced diffusion restriction is associated with coagulative necrosis surrounded by viable tumor and decreased overall survival in patients with recurrent glioblastoma. Am J Neuroradiol 2016; 37:2201–2208.

82. Detsky JS, Keith J, Conklin J, *et al.* Differentiating radiation necrosis from tumor progression in brain metastases treated with stereotactic radiotherapy: utility of intravoxel incoherent motion perfusion MRI and correlation with histopathology. J Neurooncol 2017; 134:433–441.

83. ■ Schwarz D, Bendszus M, Breckwoldt MO. Clinical value of susceptibility weighted imaging of brain metastases. Front Neurol 2020; 11:55.

This article underscore the importance of susceptibility weighted imaging during treatment monitoring.

84. Mohammed W, Xunning H, Haibin S, Jingzhi M. Clinical applications of susceptibility-weighted imaging in detecting and grading intracranial gliomas: a review. Cancer Imaging 2013; 13:186–195.

85. Park MJ, Kim HS, Jahng G-H, *et al.* Semiquantitative assessment of intratumoral susceptibility signals using non-contrast-enhanced high-field high-resolution susceptibility-weighted imaging in patients with gliomas: comparison with MR perfusion imaging. Am J Neuroradiol 2009; 30:1402–1408.

86. Varon D, Simons M, Chiang F, *et al.* Brain radiation-related black dots on susceptibility-weighted imaging. Neuroradiol J 2014; 27:445–451.

87. Kim T-H, Yun TJ, Park C-K, *et al.* Combined use of susceptibility weighted magnetic resonance imaging sequences and dynamic susceptibility contrast perfusion weighted imaging to improve the accuracy of the differential diagnosis of recurrence and radionecrosis in high-grade glioma patients. Oncotarget 2017; 8:20340–20353.

88. Belliveau J-G, Bauman GS, Macdonald D, *et al.* Apparent transverse relaxation (R2∗) on MRI as a method to differentiate treatment effect (pseudoprogression) versus progressive disease in chemoradiation for malignant glioma. J Med Imaging Radiat Oncol 2018; 62:224–231.

89. Belliveau J-G, Jensen MD, Stewart JMP, *et al.* Prediction of radiation necrosis in a rodent model using magnetic resonance imaging apparent transverse relaxation ($R_{2}^{∗}$). Phys Med Biol 2018; 63:035010.

90. Filss CP, Cicone F, Shah NJ, *et al.* Amino acid PET and MR perfusion imaging in brain tumours. Clin Transl Imaging 2017; 5:209–223.

91. Galldiks N, Kocher M, Ceccon G, *et al.* Imaging challenges of immunotherapy and targeted therapy in patients with brain metastases: response, progression, and pseudoprogression. Neuro-Oncol 2020; 22:17–30.

92. Kaufmann TJ, Smits M, Boxerman J, *et al.* Consensus recommendations for a standardized brain tumor imaging protocol for clinical trials in brain metastases. Neuro-Oncol 2020; 22:757–772.

93. Wan B, Wang S, Tu M, *et al.* The diagnostic performance of perfusion MRI for differentiating glioma recurrence from pseudoprogression: a meta-analysis. Medicine (Baltimore) 2017; 96:e6333.

94. Hoefnagels FWA, Lagerwaard FJ, Sanchez E, *et al.* Radiological progression of cerebral metastases after radiosurgery: assessment of perfusion MRI for differentiating between necrosis and recurrence. J Neurol 2009; 256:878–887.

95. Kong D-S, Kim ST, Kim E-H, *et al.* Diagnostic dilemma of pseudoprogression in the treatment of newly diagnosed glioblastomas: the role of assessing relative cerebral blood flow volume and oxygen-6-methylguanine-DNA methyltransferase promoter methylation status. Am J Neuroradiol 2011; 32:382–387.

96. Mitsuya K, Nakasu Y, Horiguchi S, *et al.* Perfusion weighted magnetic resonance imaging to distinguish the recurrence of metastatic brain tumors from radiation necrosis after stereotactic radiosurgery. J Neurooncol 2010; 99:81–88.

97. Roberts HC, Roberts TP, Brasch RC, Dillon WP. Quantitative measurement of microvascular permeability in human brain tumors achieved using dynamic contrast-enhanced MR imaging: correlation with histologic grade. AJNR Am J Neuroradiol 2000; 21:891–899.

98. Spampinato MV, Schiarelli C, Cianfoni A, *et al.* Correlation between cerebral blood volume measurements by perfusion-weighted magnetic resonance imaging and two-year progression-free survival in gliomas. Neuroradiol J 2013; 26:385–395.

99. Smits M. Imaging of oligodendroglioma. Br J Radiol 1060; 89:20150857.

100. Essig M, Waschkies M, Wenz F, *et al.* Assessment of brain metastases with dynamic susceptibility-weighted contrast-enhanced MR imaging: initial results. Radiology 2003; 228:193–199.

101. Schmainda KM, Prah M, Connelly J, *et al.* Dynamic-susceptibility contrast agent MRI measures of relative cerebral blood volume predict response to bevacizumab in recurrent high-grade glioma. Neuro-Oncol 2014; 16:880–888.

102. Bisdas S, Kirkpatrick M, Giglio P, *et al.* Cerebral blood volume measurements by perfusion-weighted MR imaging in gliomas: ready for prime time in predicting short-term outcome and recurrent disease? Am J Neuroradiol 2009; 30:681–688.

103. Barajas RF, Chang JS, Sneed PK, *et al.* Distinguishing recurrent intra-axial metastatic tumor from radiation necrosis following gamma knife radiosurgery using dynamic susceptibility-weighted contrast-enhanced perfusion MR imaging. Am J Neuroradiol 2009; 30:367–372.

104. van Dijken BRJ, van Laar PJ, Smits M, *et al.* Perfusion MRI in treatment evaluation of glioblastomas: clinical relevance of current and future techniques. J Magn Reson Imaging 2019; 49:11–22.

105. Strauss SB, Meng A, Ebani EJ, Chiang GC. Imaging glioblastoma posttreatment. Neuroimaging Clin N Am 2021; 31:103–120.

106. Cao Y. The promise of dynamic contrast-enhanced imaging in radiation therapy. Semin Radiat Oncol 2011; 21:147–156.

107. Narang J, Jain R, Arbab AS, *et al.* Differentiating treatment-induced necrosis from recurrent/progressive brain tumor using nonmodel-based semiquantitative indices derived from dynamic contrast-enhanced T1-weighted MR perfusion. Neuro-Oncol 2011; 13:1037–1046.

108. Thomas AA, Arevalo-Perez J, Kaley T, *et al.* Dynamic contrast enhanced T1 MRI perfusion differentiates pseudoprogression from recurrent glioblastoma. J Neurooncol 2015; 125:183–190.

109. Winter JD, Moraes FY, Chung C, Coolens C. Detectability of radiation-induced changes in magnetic resonance biomarkers following stereotactic radiosurgery: a pilot study. PLoS One 2018; 13:e0207933.

110. Morabito R, Alafaci C, Pergolizzi S, *et al.* DCE and DSC perfusion MRI diagnostic accuracy in the follow-up of primary and metastatic intra-axial

brain tumors treated by radiosurgery with cyberknife. Radiat Oncol Lond Engl 2019; 14:65.
111. Seeger A, Braun C, Skardelly M, *et al.* Comparison of three different MR perfusion techniques and MR spectroscopy for multiparametric assessment in distinguishing recurrent high-grade gliomas from stable disease. Acad Radiol 2013; 20:1557–1565.
112. Zakhari N, Taccone MS, Torres CH, *et al.* Prospective comparative diagnostic accuracy evaluation of dynamic contrast-enhanced (DCE) vs. dynamic susceptibility contrast (DSC) MR perfusion in differentiating tumor recurrence from radiation necrosis in treated high-grade gliomas. J Magn Reson Imaging JMRI 2019; 50:573–582.
113. Haller S, Zaharchuk G, Thomas DL, *et al.* Arterial spin labeling perfusion of the brain: emerging clinical applications. Radiology 2016; 281:337–356.
114. Xu Q, Liu Q, Ge H, *et al.* Tumor recurrence versus treatment effects in glioma: a comparative study of three dimensional pseudo-continuous arterial spin labeling and dynamic susceptibility contrast imaging. Medicine (Baltimore) 2017; 96:e9332.
115. Kazda T, Bulik M, Pospisil P, *et al.* Advanced MRI increases the diagnostic accuracy of recurrent glioblastoma: single institution thresholds and validation of MR spectroscopy and diffusion weighted MR imaging. NeuroImage Clin 2016; 11:316–321.
116. Kamada K, Houkin K, Abe H, *et al.* Differentiation of cerebral radiation necrosis from tumor recurrence by proton magnetic resonance spectroscopy. Neurol Med Chir (Tokyo) 1997; 37:250–256.
117. Verma N, Cowperthwaite MC, Burnett MG, Markey MK. Differentiating tumor recurrence from treatment necrosis: a review of neuro-oncologic imaging strategies. Neuro-Oncol 2013; 15:515–534.
118. Raimbault A, Cazals X, Lauvin M-A, *et al.* Radionecrosis of malignant glioma and cerebral metastasis: a diagnostic challenge in MRI. Diagn Interv Imaging 2014; 95:985–1000.
119. Zhang H, Ma L, Wang Q, *et al.* Role of magnetic resonance spectroscopy for the differentiation of recurrent glioma from radiation necrosis: a systematic review and meta-analysis. Eur J Radiol 2014; 83:2181–2189.
120. Weybright P, Sundgren PC, Maly P, *et al.* Differentiation between brain tumor recurrence and radiation injury using MR spectroscopy. AJR Am J Roentgenol 2005; 185:1471–1476.
121. Huang J, Wang A-M, Shetty A, *et al.* Differentiation between intra-axial metastatic tumor progression and radiation injury following fractionated radiation therapy or stereotactic radiosurgery using MR spectroscopy, perfusion MR imaging or volume progression modeling. Magn Reson Imaging 2011; 29:993–1001.
122. Chuang M-T, Liu Y-S, Tsai Y-S, *et al.* Differentiating radiation-induced necrosis from recurrent brain tumor using MR perfusion and spectroscopy: a meta-analysis. PLoS One 2016; 11:e0141438.
123. Branzoli F, Marjańska M. Magnetic resonance spectroscopy of isocitrate dehydrogenase mutated gliomas: current knowledge on the neurochemical profile. Curr Opin Neurol 2020; 33:413–421.
124. Dang L, White DW, Gross S, *et al.* Cancer-associated IDH1 mutations produce 2-hydroxyglutarate. Nature 2009; 462:739–744.
125. Andronesi OC, Loebel F, Bogner W, *et al.* Treatment response assessment in IDH-mutant glioma patients by noninvasive 3D functional spectroscopic mapping of 2-hydroxyglutarate. Clin Cancer Res 2016; 22:1632–1641.
126. Choi C, Raisanen JM, Ganji SK, *et al.* Prospective longitudinal analysis of 2-hydroxyglutarate magnetic resonance spectroscopy identifies broad clinical utility for the management of patients with *IDH* -mutant glioma. J Clin Oncol 2016; 34:4030–4039.
127. Soni N, Priya S, Bathla G. Texture analysis in cerebral gliomas: a review of the literature. Am J Neuroradiol 2019; 40:928–934.
128. Varghese BA, Cen SY, Hwang DH, Duddalwar VA. Texture analysis of imaging: what radiologists need to know. Am J Roentgenol 2019; 212:520–528.
129. Larroza A, Bodí V, Moratal D. Texture analysis in magnetic resonance imaging: review and considerations for future applications. Assessment of cellular and organ function and dysfunction using direct and derived MRI methodologies.2016IntechOpen.
130. Lambin P, Rios-Velazquez E, Leijenaar R, *et al.* Radiomics: extracting more information from medical images using advanced feature analysis. Eur J Cancer 2012; 48:441–446.
131. Ismail M, Hill V, Statsevych V, *et al.* Shape features of the lesion habitat to differentiate brain tumor progression from pseudoprogression on routine multiparametric MRI: a multisite study. Am J Neuroradiol 2018; 39: 2187–2193.
132. Paprottka KJ, Kleiner S, Preibisch C, *et al.* Fully automated analysis combining [18F]-FET-PET and multiparametric MRI including DSC perfusion and APTw imaging: a promising tool for objective evaluation of glioma progression. Eur J Nucl Med Mol Imaging 2021; 1–11.
133. Smits M. MRI biomarkers in neuro-oncology. Nat Rev Neurol 2021; ■■ 1–15.
This excellent up-do-date article explains the current role of MRI in neuro-oncology, with a focus on advanced quantitative bio-markers and radiomics.
134. Deshmane A, Zaiss M, Lindig T, *et al.* 3D gradient echo snapshot CEST MRI with low power saturation for human studies at 3T. Magn Reson Med 2019; 81:2412–2423.
135. Togao O, Keupp J, Hiwatashi A, *et al.* Amide proton transfer imaging of brain tumors using a self-corrected 3D fast spin-echo dixon method: comparison with separate B_0 correction: 3D FSE Dixon APT imaging of brain tumor. Magn Reson Med 2017; 77:2272–2279.
136. Wu B, Warnock G, Zaiss M, *et al.* An overview of CEST MRI for non-MR physicists. EJNMMI Phys 2016; 3:19.
137. Stancanello J, Terreno E, Castelli DD, *et al.* Development and validation of a smoothing-splines-based correction method for improving the analysis of CEST-MR images. Contrast Media Mol Imaging 2008; 3:136–149.
138. Windschuh J, Zaiss M, Meissner J-E, *et al.* Correction of *B* 1-inhomogeneities for relaxation-compensated CEST imaging at 7 T: correction of B1-inhomogeneities for relaxation-compensated CEST imaging at 7 T. NMR Biomed 2015; 28:529–537.
139. Breitling J, Deshmane A, Goerke S, *et al.* Adaptive denoising for chemical exchange saturation transfer MR imaging. NMR Biomed 2019; 32:e4133.
140. Terreno E, Stancanello J, Longo D, *et al.* Methods for an improved detection of the MRI-CEST effect. Contrast Media Mol Imaging 2009; 4:237–247.
141. Togao O, Yoshiura T, Keupp J, *et al.* Amide proton transfer imaging of adult diffuse gliomas: correlation with histopathological grades. Neuro-Oncol 2014; 16:441–448.
142. Kim M, Torrealdea F, Adeleke S, *et al.* Challenges in glucoCEST MR body imaging at 3 Tesla. Quant Imaging Med Surg 2019; 9:1628–1640.
143. Jones KM, Randtke EA, Yoshimaru ES, *et al.* Clinical translation of tumor acidosis measurements with AcidoCEST MRI. Mol Imaging Biol 2017; 19:617–625.
144. Jones KM, Pollard AC, Pagel MD. Clinical applications of chemical exchange saturation transfer (CEST) MRI: clinical applications of CEST MRI. J Magn Reson Imaging 2018; 47:11–27.
145. Zhao X, Wen Z, Zhang G, *et al.* Three-dimensional turbo-spin-echo amide proton transfer MR imaging at 3-Tesla and its application to high-grade human brain tumors. Mol Imaging Biol 2013; 15:114–122.
146. Zhou J, Zhu H, Lim M, *et al.* Three-dimensional amide proton transfer MR imaging of gliomas: initial experience and comparison with gadolinium enhancement: 3D APT Imaging of Gliomas. J Magn Reson Imaging 2013; 38:1119–1128.
147. Jiang S, Eberhart CG, Zhang Y, *et al.* Amide proton transfer-weighted magnetic resonance image-guided stereotactic biopsy in patients with newly diagnosed gliomas. Eur J Cancer 2017; 83:9–18.
148. Jiang S, Zou T, Eberhart CG, *et al.* Predicting IDH mutation status in grade II gliomas using amide proton transfer-weighted (APTw) MRI: predicting IDH Status With APTw MRI. Magn Reson Med 2017; 78:1100–1109.
149. Ma B, Blakeley JO, Hong X, *et al.* Applying amide proton transfer-weighted MRI to distinguish pseudoprogression from true progression in malignant gliomas: APT-MRI of Pseudo- vs. true progression. J Magn Reson Imaging 2016; 44:456–462.
150. Casagranda S, Mancini L, Gautier G, *et al.* Fluid suppression in CEST imaging affects predominantly IDH-mutant 1p/19q retained gliomas with T2-FLAIR mismatch. In: ISMRM 29th Annual Meeting Virtual Conference and Exhibition. 2020.
151. Mancini L, Casagranda S, Torrealdea F, *et al.* (2020) Glioma staging with CEST asymmetry curves and amides/amines ratio. In: ISMRM 29th Annual Meeting Virtual Conference and Exhibition. 2020.
152. Zhou J, Tryggestad E, Wen Z, *et al.* Differentiation between glioma and radiation necrosis using molecular magnetic resonance imaging of endogenous proteins and peptides. Nat Med 2011; 17:130–134.
153. Hong X, Liu L, Wang M, *et al.* Quantitative multiparametric MRI assessment of glioma response to radiotherapy in a rat model. Neuro-Oncol 2014; 16:856–867.
154. Jiang S, Eberhart CG, Lim M, *et al.* Identifying recurrent malignant glioma after treatment using amide proton transfer-weighted MR imaging: a validation study with image-guided stereotactic biopsy. Clin Cancer Res 2019; 25:552–561.
155. Park JE, Kim HS, Park SY, *et al.* Identification of early response to anti-angiogenic therapy in recurrent glioblastoma: amide proton transfer–weighted and perfusion-weighted MRI compared with diffusion-weighted MRI. Radiology 2020; 295:397–406.
156. Schön S, Cabello J, Liesche-Starnecker F, *et al.* Imaging glioma biology: spatial comparison of amino acid PET, amide proton transfer, and perfusion-weighted MRI in newly diagnosed gliomas. Eur J Nucl Med Mol Imaging 2020; 47:1468–1475.
157. Goerke S, Zaiss M, Kunz P, *et al.* Signature of protein unfolding in chemical exchange saturation transfer imaging: SIGNATURE OF PROTEIN UNFOLDING IN CEST. NMR Biomed 2015; 28:906–913.
158. Mehrabian H, Desmond KL, Soliman H, *et al.* Differentiation between radiation necrosis and tumor progression using chemical exchange saturation transfer. Clin Cancer Res 2017; 23:3667–3675.
159. Goerke S, Breitling J, Korzowski A, *et al.* Clinical routine acquisition protocol for 3D relaxation-compensated APT and rNOE CEST-MRI of the human brain at 3T. Magn Reson Med 2021; 86:393–404.

